CSIRO PUBLISHING

International Journal of Wildland Fire **2017**, *26*, 393–398
http://dx.doi.org/10.1071/WF16130

Incorporating fine-scale drought information into an eastern US wildfire hazard model

Matthew P. Peters[A,B] *and Louis R. Iverson*[A]

[A]USDA Forest Service, Northern Research Station, 359 Main Road, Delaware, OH 43015, USA.
[B]Corresponding author. Email: matthewpeters@fs.fed.us

Abstract. Wildfires in the eastern United States are generally caused by humans in locations where human development and natural vegetation intermingle, e.g. the wildland–urban interface (WUI). Knowing where wildfire hazards are elevated across the forested landscape may help land managers and property owners plan or allocate resources for potential wildfire threats. In an earlier paper, we presented a model showing monthly hazards of wildfire across Ohio, Pennsylvania and New Jersey at a 30-m resolution. Here, we refine the spatial resolution of drought conditions by incorporating a 4 × 4-km gridded self-calibrated drought index, include mean winter temperature to restrict hazards from being modelled into locations possibly covered by snow, and compare the performance of the updated models with the original ones. The area under the curve values for the updated models were within 10% of the values for the original models, but the refinement of drought conditions resulted in a less generalised probability of hazards, potentially increasing the applicability of these models. Among the 12 monthly models, the wildland–urban interface had the highest contribution followed by a weighed drought frequency index.

Additional keywords: cumulative drought severity index (CDSI), hazard mapping, Maxent, New Jersey, Ohio, Pennsylvania.

Received 20 July 2016, accepted 17 February 2017, published online 27 March 2017

Introduction

Droughts can increase fuel loads by causing tree mortality (Park Williams *et al.* 2013; Clark *et al.* 2016) and can create conditions of low humidity that dry woody debris and forest litter, potentially increasing fire ignition and spread (Gill 1983; Ruthrof *et al.* 2016). Thus, wildfire hazard models have incorporated information about drought conditions to account for this influence (Bradstock *et al.* 2009; Peters *et al.* 2013*a*). We developed a predictive wildfire hazard model that indicates the long-term likelihood of wildfire occurrence (for further details see Peters *et al.* 2013*a*) using maximum entropy models parameterised with forest cover, an integrated soil moisture index (IMI), drought occurrences, and wildland–urban interface (WUI) data. Reported wildfires (≥0.1 ha of burned area) from 2000 to 2009 within the states of New Jersey, Ohio and Pennsylvania were used to estimate the monthly probability of wildfire occurrence.

One of the more widely used drought indices for ecological modelling is Palmer's Drought Severity Index (PDSI) (Palmer 1965; Dai 2011), a standardised measure of the cumulative departure in surface water demand and supply. Since its development, the PDSI has been updated by Heddinghaus and Sabol (1991) to address issues of spatial comparability raised by Alley (1984). More recently, PDSI has been calibrated to site-specific conditions to account for local climate trends and allow comparisons among regions (Wells *et al.* 2004).

Within the United States, PDSI data are often reported at climate divisions – subdivisions of each state into 10 or fewer units, often defined by county lines (Guttman and Quayle 1996). Drought and moisture conditions are averaged among weather stations within divisions to account for missing observations, and studies linking wildfires to regional drought (Miranda *et al.* 2012; Labosier *et al.* 2015) have use these aggregated meteorological records. However, methods to prepare high-resolution spatially and temporally consistent gridded meteorological datasets that overcome some of the limitations of the climate division data, specifically the averaging of conditions across large areas, are available (Abatzoglou 2013). Gridded datasets from sources such as the PRISM Climate Group, which interpolate values among observations using a Parameter-elevation Regressions on Independent Slopes Model (PRISM) (Daly *et al.* 2008), have been used in many applications (Abatzoglou and Kolden 2011; Peters *et al.* 2015) to provide a continuous climate surface based on observed data.

With datasets like PRISM providing monthly estimates of precipitation and temperature values interpolated to a resolution of 2.5′ (4 × 4 km), we processed a self-calibrated PDSI (scPDSI) algorithm to incorporate finer-resolution drought conditions into our wildfire hazard model. We anticipated that increasing the spatial resolution of drought occurrences from climate divisions to 16-km^2 grids might improve the monthly wildfire hazard models parameterised with reported wildfires from 2000 to 2009. Additionally, we evaluated whether a snowmelt function incorporated into the scPDSI algorithm performed better than models parameterised with mean winter temperature along with the other four variables (forest cover, IMI, drought occurrence and WUI) for December, January and February to account for potential snow cover.

Methods

We used a maximum entropy model (Maxent) to predict monthly wildfire hazards defined as the probability of a wildfire occurring in our study region (New Jersey, Ohio and Pennsylvania). This region is topographically diverse, with rolling hills to the west transitioning to ridge-and-valley in south-western Ohio and eastern Pennsylvania, to the Appalachian Mountains and the coastline of the Atlantic Ocean in New Jersey. The landscape is predominately 48% temperate forest, 25% agricultural and 17% developed. The models were parameterised with monthly frequencies of drought, an integrated moisture index of soil, the percentage of forest cover and wildland–urban interface classes (Peters *et al.* 2013*a*), which we updated to include fine-scale drought occurrence data. Maxent has been widely used to estimate (i.e. predict) the probability of presence for species (Hernandez *et al.* 2008; Phillips and Dudík 2008; Williams *et al.* 2009) and wildfire hazard or risk (Parisien *et al.* 2012; Bar Massada *et al.* 2013; Peters *et al.* 2013*a*). Maxent methods are advantageous for presence-only datasets (Elith *et al.* 2011) such as reported wildfires.

Climate data

Monthly interpolated climate values of precipitation and mean temperature obtained from 16-km^2 PRISM data (PRISM Climate Group 2012) for the period 1981–2010 were used to parameterise a self-calibrated PDSI algorithm (Wells *et al.* 2004). The average mean winter temperature (December, January and February) resampled to 30 m was used to parameterise corresponding monthly models to account for potential snow cover, assuming that wildfires are not likely to occur where temperatures are near-freezing. During these months, much of the region can be wet or covered in snow, preventing wildfire ignition and spread. We realise that climatic conditions in this region can be influenced by topography and resampling to 30 m could result in a homogenisation of modelled hazard potential; however, the variations are likely small at the monthly scale.

Palmer Drought Severity Index

An algorithm to calculate scPDSI values (Wells *et al.* 2004) that processes 25+ years of climate data for a specific location was incorporated into a geoprocessing script. Parameters for self-calibration include latitude, available water supply (AWS) of the soil, monthly climate normal (e.g. mean temperature of period), monthly precipitation and mean temperature. A snowmelt function (Yan *et al.* 2014) that accumulates a snowpack when monthly temperatures are $\leq 0°C$ and precipitation >0 mm and then releases a portion of the snowpack when monthly temperatures are above freezing was used to alter monthly precipitation values. Individual output files for each grid were compiled into a regional dataset, and the frequency of drought conditions was combined into a cumulative drought severity index (CDSI) (Peters *et al.* 2015). CDSI is the weighted sum of monthly occurrences, calculated for each 16-km^2 cell, for moderate (-2.0 to -2.99), severe (-3.0 to -3.99) and extreme (≤ -4.0) drought conditions multiplied by 1, 2 and 3 respectively.

Drought conditions were calculated using climate data obtained from the PRISM Climate Group (2012) and processed for each 16-km^2 grid centroid. Soil AWS (mm) was obtained from the county soil survey geographic (SSURGO) database (NRCS 2009) and prepared using methods described by Peters *et al.* (2013*b*). Mean AWS to a depth of 150 cm was aggregated from 30-m data to each 16-km^2 PRISM grid. The snowmelt function adds monthly precipitation to a snowpack if temperature is $\leq 0°C$ and thereby alters monthly precipitation values. Precipitation stored in the snowpack is released by 20% of the monthly temperature when $0°C <$ temperature $\leq 5°C$; otherwise, the entire snowpack is added to the monthly precipitation corresponding to temperatures exceeding the 5°C threshold.

Wildfire hazard model

The Maxent models use four environmental conditions, CDSI, IMI, percentage forest cover and WUI classes, to predict the monthly probability of occurrence for reported wildfires during the period from 2000 to 2009 (see Section S1 of online supplementary material for details of predictors). The weighted monthly cumulative occurrence of scPDSI values indicating drought conditions (scPDSI < -1.99) for the 10 months of data (i.e. January of 2000 to 2009) provides a measure of recent drought occurrence and severity that aims to represent the relative hazard for this period. The calculation of IMI (Iverson *et al.* 1997), which had been modified to include an infinite directional flow accumulation algorithm (Tarboton 1997), provides a measure of long-term potential soil moisture. Percentage of forest cover obtained from LANDFIRE (2007) data helps differentiate forested land from non-forested land. WUI classes were obtained from the Spatial Analysis for Conservation and Sustainability (SILVIS Laboratory) at the University of Wisconsin–Madison and are based on data from the 2000 Census and 1992 National Land Cover Dataset (Radeloff *et al.* 2005). This component integrates land use and land cover with human population density and provides a measure of how intermingled humans are within and among forested landscapes. Both IMI and forest cover had native resolutions of 30 m, whereas values of CDSI were resampled from 16-km^2 grids and WUI rasterised from a vector dataset.

Models developed by Peters *et al.* (2013*a*) were run for the present study using the same parameters, but with CDSI based on scPDSI values instead of the Climate Division data used to calculate monthly drought frequencies. A total of 4847 wildfires were reported over the 10-year period, and for each month, 10 iterations were run using 75% of the data to train and 25% to test the models. An additional 527 records from 2010 were used for evaluation. Additionally, new models were developed for December, January and February that included: (1) CDSI values based on scPDSI run without the snowmelt function, and (2) mean winter temperatures.

Model evaluation

Results from the original models using climate division PDSI drought frequency (hereafter referred to as climate division

Table 1. Monthly mean area under the curve (AUC) values with standard deviation included in parentheses and predictor variable contribution (percentage) from 10 model iterations

Predictor variables include wildland–urban interface designation (WUI), Palmer drought severity index (PDSI), percentage forest cover (Forest), an integrated moisture index (IMI), a cumulative drought severity index (CDSI) that includes a snowmelt function, and a mean monthly temperature for Jan, Feb and Dec (T_{win})

	Climate division models					CDSI models					Winter models					
	AUC	WUI	PDSI	Forest	IMI	AUC	WUI	CDSI	Forest	IMI	AUC	WUI	CDSI	Forest	IMI	T_{win}
Jan	0.83 (0.02)	57.8	19.3	16.1	6.8	0.82 (0.03)	54.9	20.9	20.3	4.0	0.91 (0.02)	22.0	5.9	6.8	1.2	64.1
Feb	0.81 (0.02)	50.2	25.5	14.1	10.1	0.79 (0.01)	56.7	14.4	16.9	12.0	0.90 (0.01)	19.5	1.1	4.3	2.3	72.7
Mar	0.80 (0.01)	34.9	59.5	5.1	0.5	0.76 (0.01)	66.2	14.1	15.5	4.2						
Apr	0.76 (0.01)	63.2	27.6	8.4	0.8	0.75 (0.01)	71.2	17.9	9.6	1.3						
May	0.80 (0.01)	32.5	57.8	8.1	1.6	0.75 (0.01)	74.9	7.1	13.2	4.8						
Jun	0.83 (0.02)	49.2	33.3	11.3	6.3	0.82 (0.01)	49.2	30.7	12.4	7.8						
Jul	0.80 (0.02)	49.8	26.5	13.4	10.4	0.80 (0.02)	52.6	21.0	15.2	11.2						
Aug	0.87 (0.02)	8.9	80.8	6.4	3.9	0.79 (0.02)	44.2	30.3	13.5	11.9						
Sep	0.79 (0.02)	29.8	48.4	13.9	8	0.76 (0.02)	60.3	2.6	23.9	13.2						
Oct	0.89 (0.02)	43	33.4	5.6	17.9	0.77 (0.02)	55.5	15.4	8.6	20.5						
Nov	0.82 (0.01)	26.6	53.6	6.3	13.5	0.81 (0.01)	39.9	40.6	8.1	11.4						
Dec	0.86 (0.02)	36.7	34.5	7.7	21.1	0.83 (0.03)	40.9	18.9	11.2	29.1	0.90 (0.01)	17.7	1.2	3.4	9.1	68.6

models), those using a CDSI derived from 16-km^2 gridded scPDSI values (hereafter referred to as CDSI models), and the 3 months with mean winter temperature (hereafter referred to as winter models) were compared and evaluated for potential improvements. Evaluation consisted of: (1) a comparison of area under the curve (AUC) values between the three model parameterisations; (2) a comparison among monthly predicted hazard probabilities for each reported wildfire to determine which of the two (or three) models resulted in a greater likelihood of occurrence using reported fires from 2000 to 2009 and 527 fires from 2010; and (3) a visual examination of model output and comparison of areal changes.

Results

The CDSI models developed here showed slight reductions in AUC (up to 12%) across months, as compared with the climate division models (Table 1). However, the major difference between the original climate division models (Peters *et al.* 2013*a*; Fig. S1) and the CDSI models (Fig. 1) was the variation in spatial patterns resulting from the change in resolution of drought condition data as well as the weighting of drought classes to incorporate both intensity and frequency. Also different are the percentage contributions from the predictor variables, where WUI now has more of an influence in the CDSI models than PDSI (Peters *et al.* 2013*a*; Fig. S4). Winter models for December, January and February that included mean winter temperature had higher AUC values (9 to 13%) than the CDSI models that incorporated a snowmelt function, indicating that temperature was more informative for these months than the snowmelt function (Table 1). Additionally, mean winter temperature had a greater contribution (64 to 72%) among the predictor variables for these months.

The 4847 reported wildfires from 2000 to 2009 used to train monthly models and predict the probability of wildfire hazard, as well as the 527 fires from 2010 for model evaluation both had bimodal distributions that peaked in April with 1669 and 213 fires, and again in the fall with 335 fires (November) and 64 fires (October) for training and testing data respectively (Table 1). Based on the coordinates associated with the reported fires, corresponding hazard probabilities were examined among the climate division, CDSI and winter models. Using the maximum training sensitivity plus specificity logistic threshold (LT) calculated by Maxent, unique thresholds were used to determine whether monthly fires would have been detected by the corresponding models. Among the training data, 63.5 to 83.5, 59.6 to 75.0, and 72.1 to 78.8% of the reported monthly wildfires were located in cells with probabilities indicating a hazard of occurrence among the climate division, CDSI and winter models respectively (Table 2). The winter models resulted in differences of 4.9, 16.7 and 2.6% for training data associated with hazards of occurrence during the months of December, January and February respectively compared with the CDSI models. For the testing data of months in 2010 with at least five fires, the climate division models captured between 34.8 and 77.9%, whereas the CDSI models captured between 18.8 and 66.7% of wildfires. Both models had higher accuracy for the spring fires and lower accuracy for fall fires (Table 2).

In addition to using the LT to assess locations of reported fires, we compared model outputs for changes in areal extent among the three models. The winter models had the smallest area (12.9 to 16.1%) of predicted hazards probabilities within the region, whereas for some months (February, March, April, June, September and November), the predicted area of fire occurrence was quite similar between the climate division and CDSI models (Fig. S5). However, for other months (May, July, August, October, and December), the predicted area for CDSI models substantially exceeded that of climate division models, especially in May. Only in January did climate division models exceed CDSI predicted area.

Discussion

The calibration of PDSI values accounts for local patterns of climatic variability to derive spatially relevant values for the water balance coefficients rather than using the empirical data

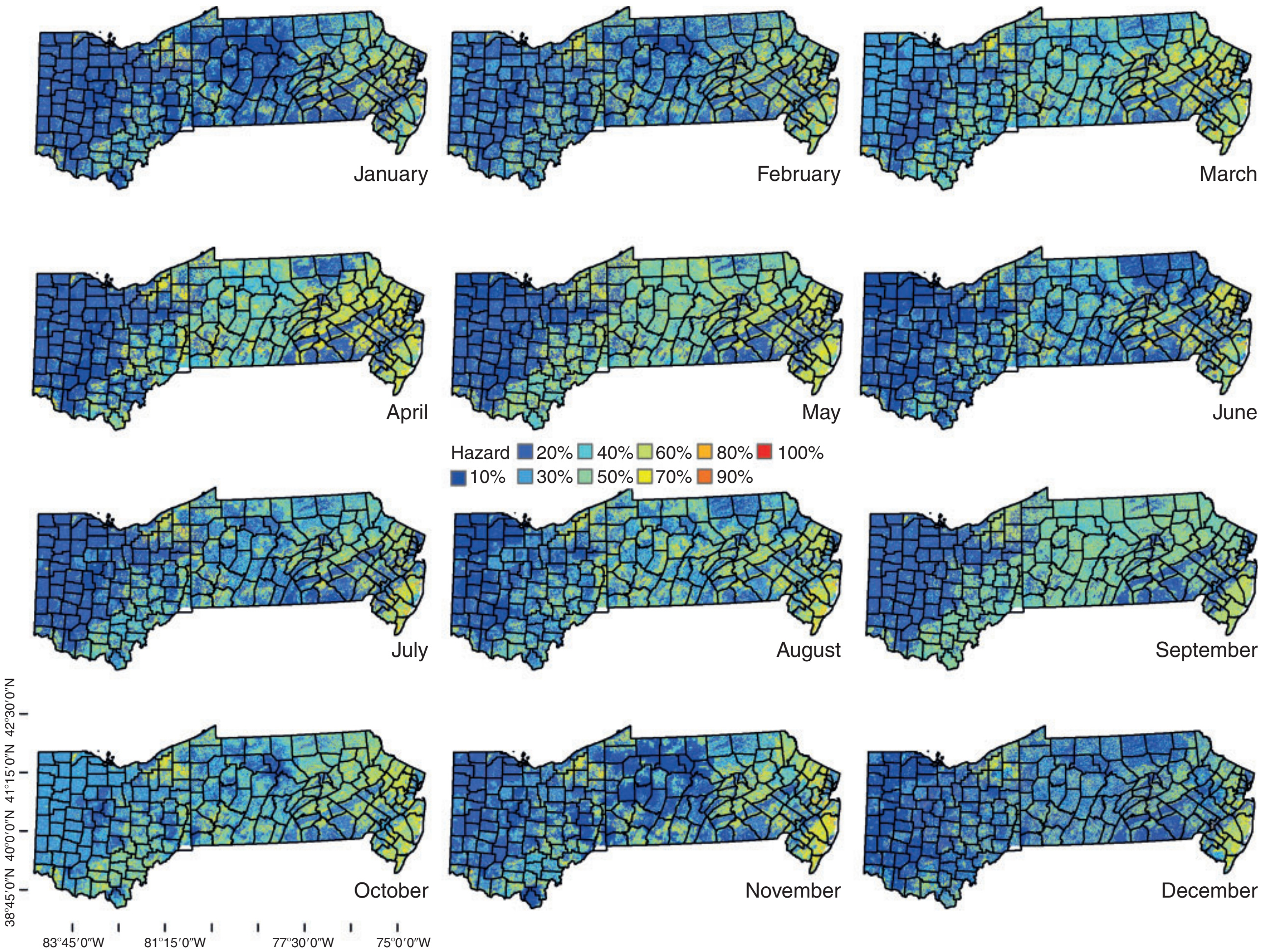

Fig. 1. Mean probability of wildfire hazard modelled using maximum entropy (10 iterations). Models were trained with monthly reported wildfires (2000–09) and four environmental datasets. Note that the spatial variation among predicted values does not resemble climate divisions as presented in Fig. S1.

from a limited set of regions (i.e. central Iowa and western Kansas) as Palmer's original equation does (Wells *et al.* 2004). In addition to the refinement gained from calibration of climatic conditions, the fine-scale information provided by a 16-km^2 gridded dataset results in a more natural spatial patterning as compared with abrupt (county) boundaries apparent in the more generalised climate division data as reported previously by Peters *et al.* (2013*a*). Because the climate divisions divide the states into 10 or fewer units, much of the region has similar drought occurrence values as opposed to the 16-km^2 grids, which are locally representative and weight the intensity of conditions. Additionally, incorporating a simple snowmelt function to alter winter and spring precipitation may also provide some realism to the February and March models despite the improvement from winter temperature with training data for February.

Based on AUC values alone, the models using cumulative weighted drought frequency (CDSI) derived from scPDSI values had a slight reduction in performance compared with the models developed with climate division drought frequency. However, the major advantage to the CDSI models is that the spatial patterns of drought have been refined to 16-km^2 grids, not the 10 or fewer climatic divisions, altering the distribution of probability of wildfire occurrence. When examining the percentage of reported wildfires coinciding with modelled probabilities $\geq$ the LT for the months of March to November, the CDSI models are within 17% of the climate division models, most of which are within 7%. The CDSI models for August and September have the greatest difference among the two parameterisations, with 16.5 and 13.9% respectively. This may be due to WUI having more of an influence in the CDSI models rather than the highly generalised drought conditions of the climate division models for these 2 months.

Differences in the contributions of predictor variables between the CDSI and climate division models indicated that drought frequency has less of an influence for the CDSI models where WUI has the greatest contribution among all months except November. In contrast, climate division models indicated drought frequency was most important for March, May, August, September and November where 73.0 to 91.8% of the region had one or more drought events. As this predictor variable was generalised across the region, it may have artificially inflated climate division model performance. The lower contribution

Table 2. Percentage of monthly reported wildfires among training and testing data above ($P \geq$ LT, captured) and below ($P <$ LT, missed) the maximum training sensitivity plus specificity logistic threshold (LT) for predicted wildfire hazards

Climate division Palmer drought severity index (PDSI) frequencies were used in the original model. A cumulative drought severity index (CDSI) was derived from self-calibrated PDSI values calculated with a snowmelt function and included in monthly Maxent models, whereas CDSI without a snowmelt function and mean winter temperature (T_{win}) were used for January, February and December. The greatest percentage of reported fires captured among the different model is indicated in boldface

		Jan	Feb	Mar	Apr	May	Jun	Jul	Aug	Sep	Oct	Nov	Dec
Training data (2000–09)	Number of fires	66	269	971	1669	620	148	184	176	166	182	335	61
	ClimDiv $P \geq$ LT	77.3	**75.8**	**71.5**	**75.8**	63.5	**73**	64.7	**83.5**	**73.5**	64.8	**78.8**	**72.1**
	ClimDiv $P <$ LT	22.7	24.2	28.5	24.2	36.5	27	35.3	16.5	26.5	35.2	21.2	27.9
	CDSI $P \geq$ LT	62.1	73.2	67.9	75	**74.2**	70.3	**67.4**	67	59.6	**72**	72.2	67.2
	CDSI $P <$ LT	37.9	26.8	32.1	25	25.8	29.7	32.6	33	40.4	28	27.8	32.8
	T_{win} $P \geq$ LT	**78.8**	**75.8**										**72.1**
	T_{win} $P <$ LT	21.2	24.2										27.9
Testing data (2010)	Number of fires	1	0	84	213	19	4	23	16	43	64	58	2
	ClimDiv $P \geq$ LT	**100**		46.4	**77.9**	47.4	**75**	34.8	**37.5**	**58.1**	59.4	**55.2**	**50**
	ClimDiv $P <$ LT	0		53.6	22.1	52.6	25	65.2	62.5	41.9	40.6	44.8	50
	CDSI $P \geq$ LT	**100**		**57.1**	66.7	**52.6**	**75**	**60.9**	18.8	48.8	**60.9**	36.2	0
	CDSI $P <$ LT	0		42.9	33.3	47.4	25	39.1	81.3	51.2	39.1	63.8	100
	T_{win} $P \geq$ LT	**100**											**50**
	T_{win} $P <$ LT	0											50

from drought frequency in the CDSI models is likely due to the higher resolution of the gridded scPDSI values, where 9.2 to 35.8% of the region had no drought and more wildfires occurring in and near WUI classes where human populations have a greater interaction with vegetation. Additionally, climate division PDSI values may not accurately reflect the true drought conditions experienced during reported fires because conditions can vary widely across large divisions (Wells *et al.* 2004; Peters *et al.* 2015).

The winter models parameterised with mean winter temperature performed better than the CDSI models with snowmelt for December through February (Table 1). Mean winter temperature had the greatest contribution among predictors for these three models and confirms that drought occurrence during this season is a poor indicator of wildfire hazards in this region. Winter temperatures were included to help restrict modelled hazards in locations typically wet or covered by snow during this period. However, accounting for snowmelt in PDSI calculations can improve early spring values by more accurately representing water supplies and deficits. Whereas snow cover will reduce fire ignitions and spread, periods of warmer than normal winter temperatures coupled with a precipitation deficit could increase the potential for wildfires in these areas. Therefore, daily conditions need to be considered when developing management practices or planning resource allocations.

Conclusions

The inclusion of high-resolution (16-km^2) drought occurrence derived from scPDSI values as a predictor of wildfire hazard produced AUC values slightly lower than models generated with coarse-resolution drought information. However, the spatial patterns resulting from the high-resolution drought occurrence data provide detail so that managers can better understand and plan for their specific area of management. These models reflect the long-term natural and anthropogenic wildfire hazards within this three-state region. Though calculation of CDSI and IMI was needed for this analysis, they are derived from nationally available data so that the process could be applied anywhere.

Predicting the influence of drought, like modelling the hazard of wildfires, is difficult because conditions can change within shorter time intervals than those used to parameterise predictive models. Our wildfire hazard models provide monthly probabilities based on reported wildfire occurrences and are meant to aid in planning and resource allocation. Managers obviously need to use current conditions in conjunction with long-term model projections as they go about their work.

Acknowledgements

We are grateful for data provided by the National Climatic Data Center and PRISM climate group. We thank Dr Hao Yan for providing code to implement the snowmelt function. We thank Matt Dickinson, Melissa Thomas-Van Grundy and Amy Scherzer and two anonymous reviewers who provided comments on an earlier version of this manuscript. Access to model outputs is available at https://doi.org/10.2737/RDS-2016-0035 (accessed 17 January 2017).

References

Abatzoglou JT (2013) Development of gridded-surface meteorological data for ecological applications and modelling. *International Journal of Climatology* **33**, 121–131. doi:10.1002/JOC.3413

Abatzoglou JT, Kolden CA (2011) Relative importance of weather and climate on wildfire growth in interior Alaska. *International Journal of Wildland Fire* **20**, 479–486. doi:10.1071/WF10046

Alley WM (1984) The Palmer Drought Severity Index: limitations and assumptions. *Journal of Climate and Applied Meteorology* **23**, 1100–1109. doi:10.1175/1520-0450(1984)023<1100:TPDSIL>2.0.CO;2

Bar Massada A, Syphard AD, Stewart SI, Radeloff VC (2013) Wildfire ignition distribution modelling: a comparative study in the Huron–Manistee National Forest, Michigan, USA. *International Journal of Wildland Fire* **22**, 174–183. doi:10.1071/WF11178

Bradstock RA, Cohn JS, Gill AM, Bedward M, Lucas C (2009) Prediction of the probability of large fires in the Sydney region of south-eastern Australia using fire weather. *International Journal of Wildland Fire* **18**, 932–943. doi:10.1071/WF08133

Clark JS, Iverson L, Woodall CW, Allen CD, Bell DM, Bragg DC, D'Amato AW, Davis FW, Hersh MH, Ibanez I, Jackson ST, Matthews S, Pederson N, Peters M, Schwartz MW, Waring KM, Zimmermann NE (2016) The impacts of increasing drought on forest dynamics, structure, and biodiversity in the United States. *Global Change Biology* **22**, 2329–2352. doi:10.1111/GCB.13160

Dai A (2011) Characteristics and trends in various forms of the Palmer Drought Severity Index during 1900–2008. *Journal of Geophysical Research* **116**, D12115. doi:10.1029/2010JD015541

Daly C, Halbleib M, Smith JI, Gibson WP, Doggett MK, Taylor GH, Curtis J, Pasteris , PP (2008) Physiographically sensitive mapping of climatological temperature and precipitation across the conterminous United States. *International Journal of Climatology* **28**, 2031–2064. doi:10.1002/JOC.1688

Elith J, Phillips SJ, Hastie T, Dudík M, Chee YE, Yates CJ (2011) A statistical explanation of MaxEnt for ecologists. *Diversity & Distributions* **17**, 43–57. doi:10.1111/J.1472-4642.2010.00725.X

Gill AM (1983) Forest fire and drought in eastern Australia. In 'Proceedings of colloquium on the significance of the Southern Oscillation Index and the need for comprehensive ocean monitoring system in Australia', 27–28 July 1983. (Australian Maritime Science Technical Advisory Committee: Canberra)

Guttman NB, Quayle RG (1996) A historical perspective of US climate divisions. *Bulletin of the American Meteorological Society* **77**, 293–303. doi:10.1175/1520-0477(1996)077<0293:AHPOUC>2.0.CO;2

Heddinghaus TR, Sabol P (1991) A review of the Palmer Drought Severity Index and where do we go from here? In 'Proceedings of the seventh conference on applied climatology', 10–13 September 1991, Salt Lake City, UT. (American Meteorological Society: Boston, MA)

Hernandez PA, Franke I, Herzog SK, Pacheco V, Paniagua L, Quintana HL, Soto A, Swenson JJ, Tovar C, Valqui TH, Vargas J, Young BE (2008) Predicting species distributions in poorly studied landscapes. *Biodiversity and Conservation* **17**, 1353–1366. doi:10.1007/S10531-007-9314-Z

Iverson LR, Dale ME, Scott CT, Prasad A (1997) A GIS-derived integrated moisture index to predict forest composition and productivity of Ohio forests (USA). *Landscape Ecology* **12**, 331–348. doi:10.1023/A:1007989813501

Labosier CF, Frauenfeld OW, Quiring SM, Lafon CW (2015) Weather type classification of wildfire ignitions in the central Gulf Coast, United States. *International Journal of Climatology* **35**, 2620–2634. doi:10.1002/JOC.4160

LANDFIRE (2007) LANDFIRE National Forest Canopy Cover layer. (USDI Geological Survey) Available at http://www.landfire.gov/ [Verified 7 January 2010]

Miranda BR, Sturtevant BR, Stewart SI, Hammer RB (2012) Spatial and temporal drivers of wildfire occurrence in the context of rural development in northern Wisconsin, USA. *International Journal of Wildland Fire* **21**, 141–154. doi:10.1071/WF10133

Natural Resources Conservation Service (NRCS) (2009) Soil Survey Geographic (SSURGO) database for counties of Alabama, Arkansas, Connecticut, Delaware, District of Columbia, Florida, Georgia, Illinois, Indiana, Iowa, Kansas, Kentucky, Louisiana, Maine, Maryland, Massachusetts, Michigan, Minnesota, Mississippi, Missouri, Nebraska, New Hampshire, New Jersey, New York, North Carolina, North Dakota, Ohio, Oklahoma, Pennsylvania, Rhode Island, South Carolina, South Dakota, Tennessee, Texas, Vermont, Virginia, West Virginia, Wisconsin. Available at https://gdg.sc.egov.usda.gov/ [Verified November 2010]

Palmer WC (1965) Meteorological drought. US Department of Commerce Weather Bureau Research Paper No. 45. Available at https://www.ncdc.noaa.gov/temp-and-precip/drought/docs/palmer.pdf [Verified 27 February 2017]

Parisien M-A, Snetsinger S, Greenberg JA, Nelson CR, Schoennagel T, Dobrowski SZ, Moritz MA (2012) Spatial variability in wildfire probability across the western United States. *International Journal of Wildland Fire* **21**, 313–327. doi:10.1071/WF11044

Park Williams A, Allen CD, Macalady AK, Griffin D, Woodhouse CA, Meko DM, Swetnam TW, Rauscher SA, Seager R, Grissino-Mayer HD, Dean JS, Cook ER, Gangodagamage C, Cai M, McDowell NG (2013) Temperature as a potent driver of regional forest drought stress and tree mortality. *Nature Climate Change* **3**, 292–297. doi:10.1038/NCLIMATE1693

Peters MP, Iverson LR, Matthews SN, Prasad AM (2013*a*) Wildfire hazard mapping: exploring site conditions in eastern US wildland–urban interfaces. *International Journal of Wildland Fire* **22**, 567–578. doi:10.1071/WF12177

Peters MP, Iverson LR, Prasad AM, Matthews SN (2013*b*) Integrating fine-scale soil data into species distribution models: preparing Soil Survey Geographic (SSURGO) data from multiple counties. USDA Forest Service, Northern Research Station, General Technical Report NRS-122. (Newtown Square, PA)

Peters MP, Iverson LR, Matthews SN (2015) Long-term droughtiness and drought tolerance of eastern US forests over five decades. *Forest Ecology and Management* **345**, 56–64. doi:10.1016/J.FORECO.2015.02.022

Phillips SJ, Dudík M (2008) Modeling of species distributions with Maxent: new extensions and a comprehensive evaluation. *Ecography* **31**, 161–175. doi:10.1111/J.0906-7590.2008.5203.X

PRISM Climate Group (2012) Parameter-elevation relationships on independent slopes model. Oregon State University. Available at http://prism.oregonstate.edu [Verified 24 February 2017]

Radeloff VC, Hammer RB, Stewart SI, Fried JS, Holcomb SS, Mckeefry JF (2005) The wildland–urban interface in the united states. *Ecological Applications* **15**, 799–805. doi:10.1890/04-1413

Ruthrof KX, Fontaine JB, Matusick G, Breshears DD, Law DJ, Powell S, Hardy G (2016) How drought-induced forest die-off alters microclimate and increases fuel loadings and fire potentials. *International Journal of Wildland Fire* . doi:10.1071/WF15028

Tarboton DG (1997) A new method for the determination of flow directions and contributing areas in grid digital elevation models. *Water Resources Research* **33**, 309–319. doi:10.1029/96WR03137

Wells N, Goddard S, Hayes MJ (2004) A self-calibrating Palmer Drought Severity Index. *Journal of Climate* **17**, 2335–2351. doi:10.1175/1520-0442(2004)017<2335:ASPDSI>2.0.CO;2

Williams JN, Seo C, Thorne J, Nelson JK, Erwin S, O'Brien JM, Schwartz MW (2009) Using species distribution models to predict new occurrences for rare plants. *Diversity & Distributions* **15**, 565–576. doi:10.1111/J.1472-4642.2009.00567.X

Yan H, Wang S-Q, Lu H-Q, Yu Q, Zhu Z-C, Myneni RB, Liu Q, Shugart HH (2014) Development of a remotely sensing seasonal vegetation-based Palmer Drought Severity Index and its application of global drought monitoring over 1982–2011. *Journal of Geophysical Research, D, Atmospheres* **119**, 9419–9440. doi:10.1002/2014JD021673